International Journal of Engineering & Technology, 7 (2.23) (2018) 459-463

International Journal of Engineering & Technology

Website: www.sciencepubco.com/index.php/IJET

Research paper

Slot Pole Study of Field Excitation Flux Switching Machines Using Segmental Rotor and Non-Overlap Windings

M. F. Omar[1]*, E. Sulaiman[2], H. A. Soomro[3], L. I. Jusoh[4], F. Amin[5]

*[1,2,3,4,5]Faculty Of Electrical And Electronic Engineering, Universiti Tun Hussein Onn Malaysia, 86400 Parit Raja, Johor, Malaysia. * [1]fairoz.Omar@Yahoo.Com, [2]erwan@Uthm.Edu.My, [3]engg.Hassansoomro@Gmail, [4]lailiiwani@Gmail.Com, [5]faisalamin1303@Gmail.Com*

Abstract

Field excitation flux switching machines (FEFSMs) in which their torque performance generated by interaction between armature and field excitation (FE) coils have been widely designed and developed for various applications. In this regard, FEFSM with salient rotor is considered the most suitable candidate for high speed applications because of their advantages of flux controllability, and robust due to single piece of rotor structure. However, the existing FEFSM with overlapped armature and FEC windings lead to increment of copper loss, motor size and material cost. In addition, the declination of torque and power densities due to high rotor weight needs to be improved. In this paper, performance comparisons of four FEFSM topologies particularly emphasis on non-overlap armature coil and FEC windings placed on the stator with segmental rotor are investigated. The performances, including flux linkage, back-emf, flux strengthening, flux line, flux distribution, cogging torque, torque and power of the proposed motor are analysed and compared using 2D finite element analysis (FEA) thru JMAG Designer version 15. As a result, segmental rotor has produced shorter flux paths, while non-overlapping windings has reduced the copper consumption. Finally, the best combination of stator slot-pole configurations is 12S-6P which provide high flux linkage, high torque and power of 0.0412 Wb, 0.77 Nm and 0.26 kW, respectively.

Keywords: *Slot pole study; Single-phase; Flux switching machine; Field excitation; Segmental rotor; Non-overlap windings.*

1. Introduction

AC machines are divided into three types: asynchronous or induction machine (IM), a synchronous machine (SM), and switch reluctance machine (SRM). Generally, main parts of the AC machine are stator, rotor and coil. Nowadays, the SM is further categorized into four types namely, field excitation SM (FESM), permanent magnet SM (PMSM), hybrid excitation SM (HESM) and flux switching machines (FSM).

FSM consists of dual salient structured brushless machine with armature coil windings and DC (field excitation coil) windings or permanent magnet in the stator [1]. Generally, the FSM motor is applied to applications that require high of torque, power and speed capabilities such as electric vehicles (EVs) [2]. The first design of FSM was introduced in 1955 and became increasingly popular among researchers due to the principle of this motor work was easier and could save manufacturing costs [3]-[6]. There are three types of FSM namely field excitation FSM (FEFSM), permanent magnet FSM (PMFSM), and hybrid excitation FSM (HEFSM).

In general, AC motors need two sources to operate, thus, all FSMs use AC as a one of source to generate flux, and torque is generated by giving second source to the motor which is either field excitation coil (FEC) or a permanent magnet (PM). Then, in the details flux sources for PMFSM is PM, and FEFSM is FEC, while both FEC and PM in HEFSM. [7]-[10]. Currently, studies on FEFSM are being conducted by researchers as their cost of construction is low and no need to worry about the ever-depleting supply of rare earth PMs.

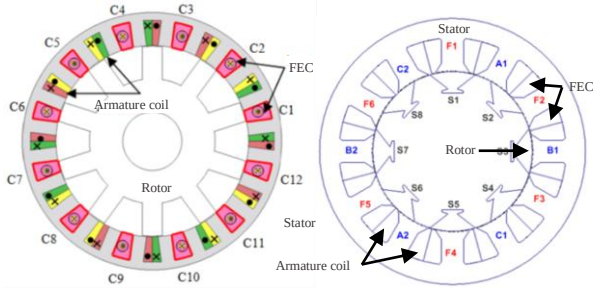

(a) (b)

Fig. 1: Example of three-phase FEFSM (a) 24S-10P salient rotor, and (b) 12S-8P segmented rotor.

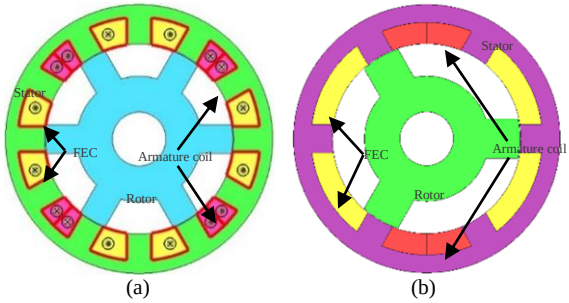

(a) (b)

Fig. 2: Previous design of single-phase FEFSM with salient rotor and overlap windings (a) 12S-6P and (b) 6S-3P.

In this regard, three-phase FEFSM with salient rotor is considered the most suitable candidate for high speed applications because of their advantages of flux controllability, and robust due to single piece of rotor structure [11], [12]. Fig. 1 shows the example of previous designs of FEFSM. Since three-phase FEFSM have high torque and power capability, this motor is not suitable for home appliances due to home appliances usually use the concept of a single-phase motor and only require low torque and power capabilities.

Consequently, the single-phase FEFSM 12S-6P and 12S-3P have been introduced as shown in Fig.2. From Fig. 2(a), the motor contains of 12 slots for armature coil and FEC windings, and 6 poles of salient rotor in the middle. The motor has advantage of less copper loss due to less copper consumption, which is four FECs winding are set in adjacent slots. Fig. 2(b) shows the 12S-3P FEFSM using salient rotor and overlap windings. This motor has a high torque and power density because less weight when compared to other single-phase FEFSM. However, the overlapping FEC and armatures windings creates the problems of high-end windings, high copper losses and less efficiency. Moreover, high rotor weight due to the salient rotor structure result in torque and power densities is reduced.

Therefore, a new structure of single-phase FEFSM using non-overlap windings between armature coil and FEC with segmental rotor structure is proposed to reduce the coil end problem as well as improve the torque and power densities. The proposed motors have twelve winding slots and six segmental rotor poles in the middle. In this paper, four single-phase FEFSMs using non-overlap windings and segmental rotor structure are presented and studied in detail. In order to determine the best performances for future analyses, analyses on flux linkage, back-emf, flux strengthening, flux line, flux distribution, torque and power have been investigated and compared.

2. Design Methodology and Specification Parameter of FEFSM

Segmental rotor dimension and work flow for designing and testing are demonstrated in Fig. 3 and Fig. 4, respectively. Only four designs of FEFSM were made by sharing the same design and condition of the stator is illustrated in Table 1. Three designs (3, 6, and 9 poles) have the same form segments with each pole having a segment span of 26 degrees, while the design with 15 poles is set to 20 degrees. Work flow for this research is divided into two parts, namely JMAG designer and JMAG geometry editor. In which, each part of the motor such as rotor, stator, armature coil and FEC are designed using JMAG geometry editor, While, materials, condition, circuit, mesh, and study properties simulation

Table 1: Design restrictions of the proposed FEFSM

Items	Dimensions			
Number of segmental rotor	3	6	9	15
Segmental span (°)	26			20
Phase number	1			
Slot number	12			
Stator outer radius (mm)	37.5			
Stator inner radius (mm)	22.5			
Stator yoke (mm)	2.5			
Stator tooth width (mm)	5			
Rotor outer radius, R_1 (mm)	22.25			
Rotor pole radius, R_2 (mm)	16.75			
Rotor inner radius, R_3 (mm)	15			
Rotor tooth width (mm)	10			
Shaft radius (mm)	15			
Air gap rotor to stator (mm)	0.25			

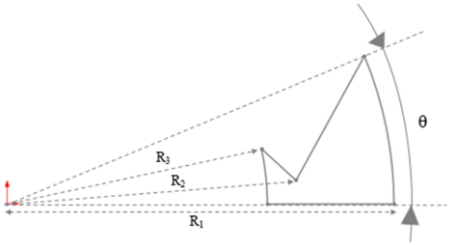

Fig. 3: Segmental rotor dimensions

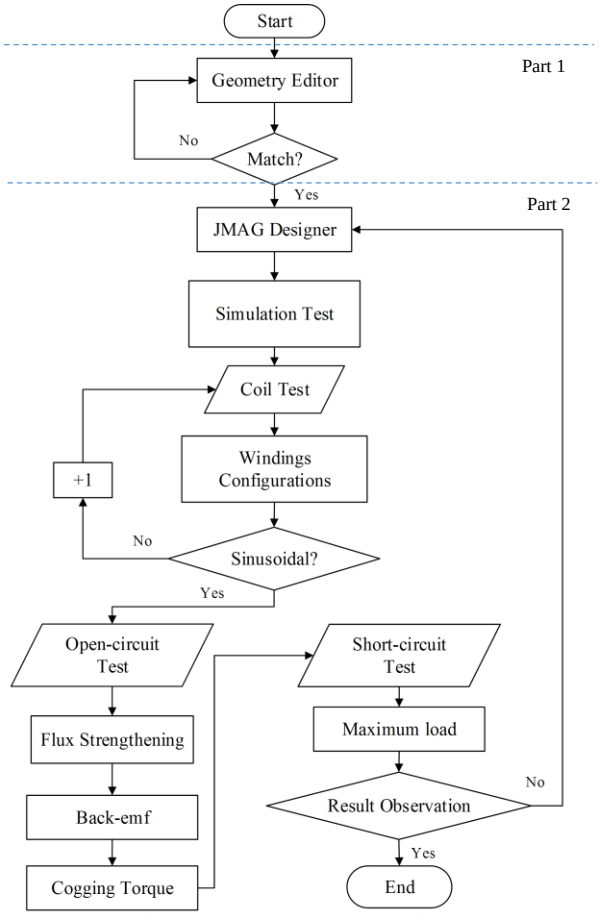

Fig. 4: Work flow for designing and testing of the proposed FEFSM

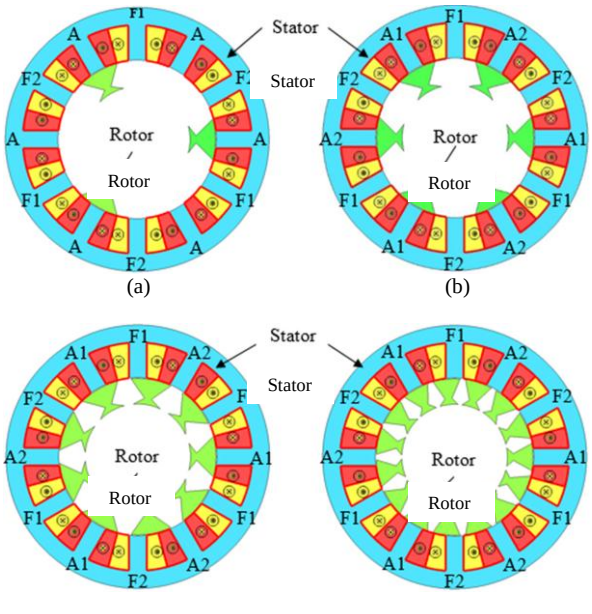

Fig. 5: Various design of the proposed FEFSM (a) 12S-3P, (b) 12S-6P, (c) 12S-9P, and (d) 12S-15P.

setting are developed by using the JMAG Designer. The possible slot poles number is defined as in Equation (1),

$$N_r = N_s[1 \pm (k/2q)] \quad (1)$$

Where *Ns* is the number of stator slot, *k* is the integer from 1 to 5, *Nr* is represented as a rotor pole number, and *q* is the number of phases. To get the right results, all FEFSM designs have shared the same stator specifications and restrictions. In open-circuit tests, only FEC receives inputs, while in short-circuit tests both armature coil and FEC are given with maximum J_A of 30 A_{rms}/mm^2 and J_E of 30 A/mm^2. The structure of proposed FEFSM designs are illustrated in Fig. 5.

3. Performance Analysis Based on 2D-FEA

3.1. Result of Flux Linkage

Basically, the FEFSM operating principle is determined by conducting a coil arrangement test. Fig. 6 demonstrates the flux linkage of all armature coils which has same polarity. From the figure, the highest flux linkage of 0.0412 Wb is achieved at 12S-6P design followed by 12S-3P, 12S-9P and 12S-15P designs with flux values of 0.0221 Wb, 0.0131 Wb and 0.0031 Wb, respectively. However, the sinusoidal flux linkage of 12S-3P design has a disruption at 140°. This situation occurs due to the high flux leakage caused by limited flux passage when the rotor at 140° as shown in Fig. 7.

3.2. Result of Flux Strengthening

For flux strengthening and weakening test, current density, J_E is set to 5 A/mm^2, 10 A/mm^2, 15 A/mm^2, 20 A/mm^2, 25 A/mm^2 and 30 A/mm^2. Then, the value of input current of FEC, I_E is calculated by using Equation (2).

$$I_E = (J_E \times \alpha \times S_E)/N_E \quad (2)$$

Where,

I_E = FEC Input current
J_E = FEC current density
α = Filling factor (set to 0.5)
N_E = FEC winding
S_E = Area of FEC slot

Fig. 8 depicts the maximum flux linkage at various FEC current density, J_E. Clearly, the highest flux of 0.0412 Wb is obtained at 12S-6P design when J_E at 30 A/mm^2. From the pattern plot, the flux shapes for 12S-3P, 12S-6P, and 12S-15P have increased linearly with increase of J_E. While for 12S-9P flux rose constantly and then decreased at FEC current density, J_E of 25 A/mm^2. This situation occurs because of flux cancelling due to some flux inside the motor flowed in the opposite direction. In addition, flux linkage of 12S-15P shows maximum flux achieved at maximum of J_E is low. This is occurred due to the high number of rotor poles have resulted in increasing number of flux paths in motor, flux break into several parts and reduces the flux strengthening.

3.3. Analysis of Back-emf

The back-emf of the proposed FEFSM at maximum J_E of 30 A/mm^2 is illustrated in Fig. 9. From the graph, clearly the highest back-emf is 12.7 V achieved from 12S-6P design, while the lowest back-emf is 3.2 V obtained from 12S-15P design. The back-emf profile for 12S-9P design is more sinusoidal than the others. While, back-emf amplitude of 7.5 V with high distortion is achieved at 12S-3P design. The total harmonic distortion (THD) versus odd harmonic order is depictured in Fig. 10. In general, all

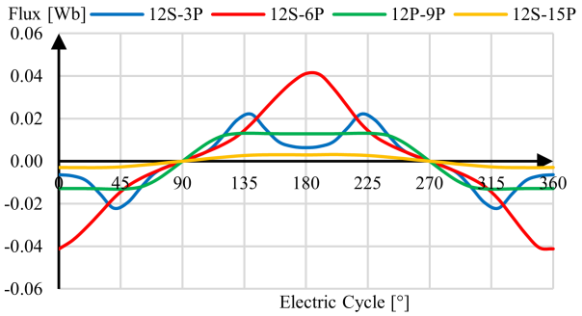

Fig. 6: FEC flux linkage at armature coils

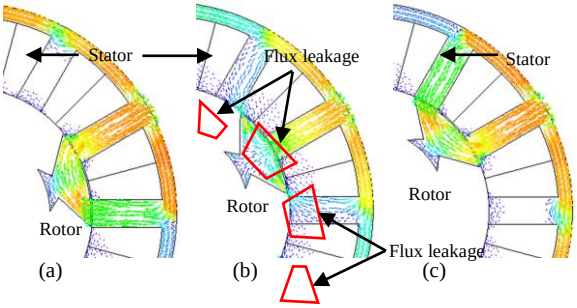

Fig. 7: Flux distribution of 12S-3P design at (a) 140°, (b) 180°, and (c) 220°.

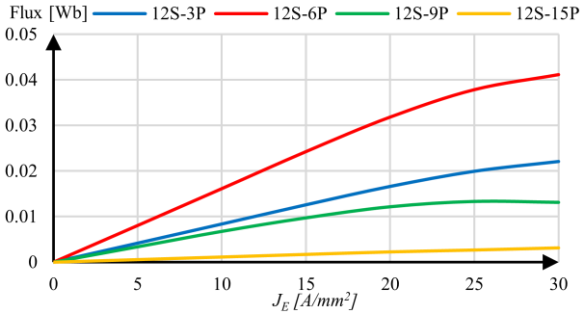

Fig. 8: Maximum flux at various J_E

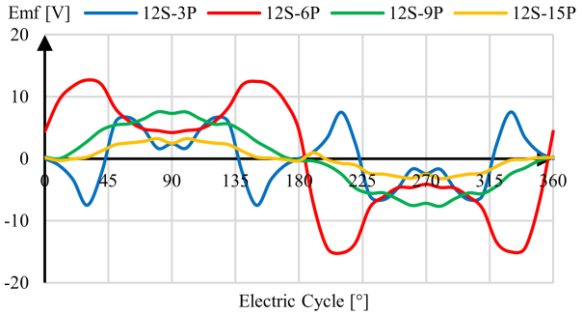

Fig. 9: Result of back-emf

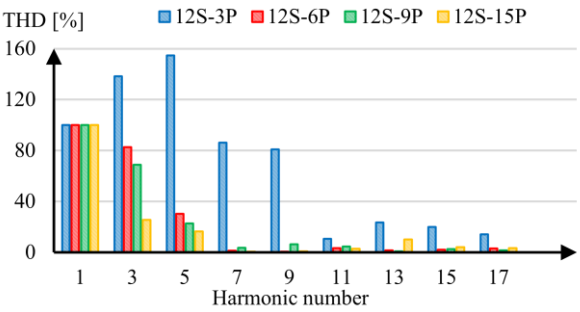

Fig. 10. Result of harmonic distortion versus odd harmonic order

designs have high interference in the 3rd and 5th harmonic. Moreover, FEFSM with 3 poles has the highest THD in all harmonic numbers, especially in 3rd and 5th order with THD magnitude of 138% and 154%, respectively. Besides, the FEFSM with 15 poles design has less disturbance on all harmonic numbers except 13th and 15th orders. Although the 6 poles design has higher distortion on the 3rd and 5th harmonic than 15 polar designs, it has low THD in all other harmonics especially in the 9th and 11th harmonics, in which the THD magnitude recorded are 0.4% in 9th order and 1.9% in 11th order.

3.4. Analysis of Flux Line

Analysis of flux line as illustrated in Fig. 11 is conducted in order to determine the flux characteristics of the proposed FEFSM. From the figure, all designs indicate a short flux line, which is a full cycle of flux occurs between two adjacent stator teeth to one rotor tooth as a red marked. 12S-6P design has the most balanced and smooth flux line on the entire magnetic part as well as less point of flux focusing as depicted in Fig 11(b). From Fig. 11(a), 12S-3P design is found has high flux focusing in the stator and rotor teeth. Ratio of 1/3 between the rotor teeth to the stator teeth has caused some of flux in stator teeth unable to flow into the rotor. The ratio of rotor to stator for 12S-9P and 12S-15P are 3/4 and 5/4, respectively. From Fig. 11(c) and 11(d), the flux focusing have occurred more on the stator and it indicates that the ratio of stator slots and rotor poles affects flux line characteristics. There are many flux focusing due to the inappropriate position of rotor and stator combinations creating various flux path and reduce the strength of flux.

3.5. Analysis of Flux Distribution

The flux distribution of various slot-pole single-phase FEFSM at maximum J_E of 30 A/mm^2 is illustrated in Fig. 12. The flux distribution was taken when the rotor at 180° electric cycle because at this point the resulting flux was highest as discussed in coil test analysis. From the figure, the best flux distribution was obtained from the 12S-6P design because of the flux leakage and magnetic part with empty flux inherent in this design is the lowest. This is aided by a combination of 6 rotor poles and 12 stator teeth allowing the flux distribution on every magnetic part of the motor to occur balanced as well as flux that flows out from the flux path becomes low. The highest flux leakage was obtained from the 12S-3P design followed by 12S-15P design. Meanwhile, 12S-9P and 12-15P designs, there are plenty of empty space on the stator yoke and stator teeth.

3.6. Result of Cogging Torque

Fig. 13 demonstrates cogging torque of the proposed FEFSM. The highest cogging torque of 3.4 Nm is obtained from 12S-6P design followed by 12S-3P design with 1.7 Nm. While, the lowest cogging torque of 0.6 Nm is achieved from 12S-15P design. In addition, cogging torque of 12S-9P is 1.03 Nm, 42% higher than 12S-15P design. Due to the concern of the disruption caused by the cogging torque, there are several techniques such as skewing, pitch notching and pole that can be applied to reduce the cogging torque to an acceptable condition.

3.7. Maximum Torque and Power

Maximum torque and power performances of the proposed FEFSM is done by giving maximum armature current density, J_A of 30 A$_{rms}$/mm^2 and FEC current density, J_E of 30 A/mm^2.
The maximum of armature current, I_A that supplied to the armature coils is calculated by using equation (3).

$$I_A = [(J_A \times \alpha \times S_A)/N_A] \times \sqrt{2} \quad (3)$$

Where,

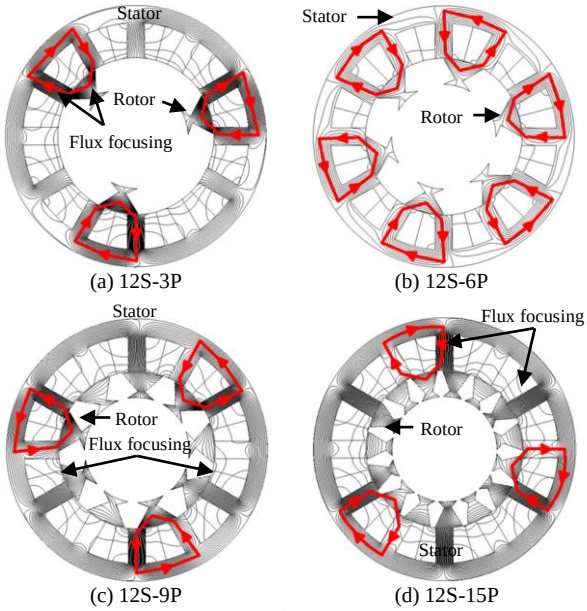

Fig. 11. Flux line of single-phase FEFSM

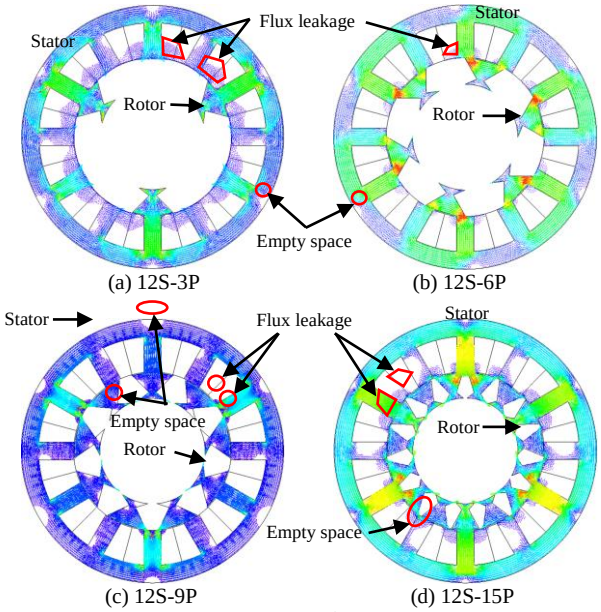

Fig. 12. Flux distribution of single-phase FEFSM

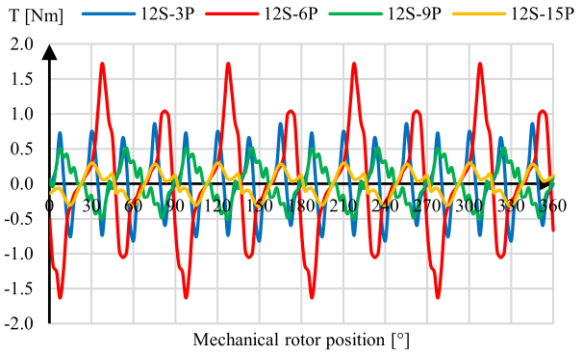

Fig. 13: Result of cogging torque

I_A = Armature input current
J_A = Armature current density
A = Filling factor (set to 0.5)
N_A = Armature turns
S_A = Area of armature slot

Fig. 14 shows the maximum torque performance of various slot poles of FEFSM. From the figure, the highest torque of 0.77 Nm is obtained from the 12S-6P design. The torque of 0.55 Nm at

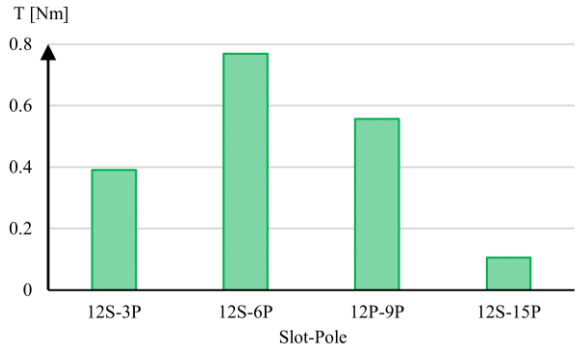

Fig. 14: Maximum torque performance of the proposed FEFSM

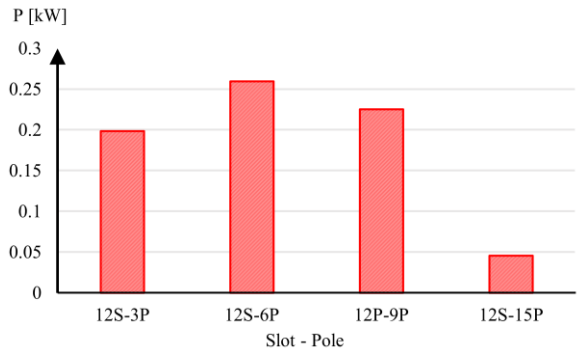

Fig. 15: Maximum power performance of the proposed FEFSM

12S-9P is 40% lower than the 12S-6P design, 41% higher than the 12S-3P design torque. While, the lowest torque of 0.11 Nm was recorded in the 12S-15P design.

Maximum power performance of the proposed FEFSM is illustrated in Fig. 15. The performance of power is obtained by using Equation (4), in which power, P is directly proportional to the torque, τ and speed, n_s.

$$P = [(2\pi)/60] \times \tau \times n_s \quad (3)$$

Obviously, the highest power of 0.26 kW was recorded from the 12S-6P design, almost 6 times higher than maximum power of 12S-3P. While, 12S-9P and 12S-3P designs have recorded maximum power of 0.23 kW and 0.2 kW respectively.

4. Conclusion

This paper presents impact of slot pole number on the characteristics of single-phase FEFSM specifically12S-3P, 12S-6P, 12S-9P and 12S-15P using non-overlap windings with segmental rotor. Characteristics of flux linkages, back-emf, flux strengthening, flux line, flux distribution, cogging torque, torque and power have been investigated and compared in detail. The proposed motor with segmental rotor has produced short magnetic flux path and less flux leakage, while the back-emf and cogging torque are considered reasonable and can be further improved. In conclusion, 12S-6P design can be considered as the best slot pole combination due to their significantly highest flux, torque and power performances of 0.041 Wb, 0.77 Nm and 0.26 kW, respectively.

Acknowledgement

This research work was funded by Ministry of Education Malaysia (MoE) under Fundamental Research Grant Scheme (FRGS), Vot. Number 1651 thru Universiti Tun Hussein Onn Malaysia (UTHM).

References

[1] J. H. Walker, “The theory of the inductor alternator,” J. IEE, vol.89, no.9, June 1942, pp.227-241.

[2] T. J. E. Miller, “Switched Reluctance Machines and Their Control”, Hillsboro, OH: Magna Physics, 1993.

[3] S. E. Rauch and L. J. Johnson, “Design principles of flux-switching alternators,” AIEE Trans. 74III, pp. 1261-1268, 1955.

[4] H. Pollock, C. Pollock, R. T. Walter, and B. V. Gorti, “Low cost, high power density, flux switching machines and drives for power tools,” in Conf. Rec. IEEE IAS Annu. Meeting, 2003, pp. 1451–1457.

[5] C. Pollock, H. Pollock, R. Barron, J. R. Coles, D. Moule, A. Court, and R. Sutton, “Flux-switching motors for automotive applications,” IEEE Trans. Ind. Appl., vol. 42, no. 5, pp. 1177–1184, Sep./Oct. 2006.

[6] Y. J. Zho, and Z. Q. Zhu “Comparison of low-cost single-phase wound-field switched-flux machines” Electric Machines & Drives Conference (IEMDC), 2013 IEEE International, 2013, pp. 1275 – 1282.

[7] Z. Q. Zhu, “Switched flux permanent magnet machines: Innovation continues”, in Proc. Int. Conf. on Electrical Machines and Systems (ICEMS), 2011, pp.1-10.

[8] Zhou, Y. J., Zhu, Z. Q., “Comparison of low-cost single-phase wound-field switched-flux machines”, IEEE Trans. on Ind. Appl., vol. 50, no. 5, pp. 3335-3345, Sept/Oct. 2014.

[9] E. Sulaiman, T. Kosaka, and N. Matsui, “Design optimization and performance of a novel 6-slot 5-pole PMFSM with hybrid excitation for hybrid electric vehicle”, IEEJ Trans. Ind. Appl., vol. 132, no. 2, Jan 2012, pp. 211-218.

[10] E. Sulaiman, M. F. M. Teridi, Z. A. Husin, M. Z. Ahmad, and T. Kosaka, “Performance comparison of 24S-10P and 24S-14P field excitation flux switching machine with single DC-coil polarity”, IEEE Int. Power Engineering and Optimization Conference, June 2013, pp. 46-51.

[11] Yu Chuang, Niu Shuangxia, Ho. S. L., Fu. W. N., “Magnetic Circuit Analysis for a Magnetless Double-Rotor Flux Switching Motor”, IEEE Trans. on Magn., vol. 51, no. 11, Nov. 2015, pp. 1-5.

[12] Sulaiman E., Khan F., Omar M. F., Romalan G. M., Jenal M., “Optimal Design of Wound-Field Flux Switching Machines for an All-Electric boat” International Conference on Electrical Machines (ICEM), Sept. 2016, pp. 2464-2470.